MODELING DEVELOPMENT: SPIKES OF THE SEA URCHIN

CLEMENS KÜHN[1] kuehn@molgen.mpg.de
ALEXANDER KÜHN[1] kuehn_a@molgen.mpg.de
ALBERT J. POUSTKA[1] poustka@molgen.mpg.de
EDDA KLIPP[1,2] klipp@molgen.mpg.de

[1] *Max-Planck-Institute for Molecular Genetics, Ihnestr 63-73, 14195 Berlin, Germany*
[2] *Humboldt Universität zu Berlin, Institute for Biology, Invalidenstr 42, 10115 Berlin, Germany*

Modeling of specification events during development poses new challenges to biochemical modeling. These include data limitations and a notorious absence of homeostasis in developing systems. The sea urchin is one of the best studied model organisms concerning development and a network, the Endomesoderm Network, has been proposed that is presumed to control endoderm and mesoderm specification in the embryo of *Strongylocentrotus purpuratus*. We have constructed a dynamic model of a subnetwork of the Endomesoderm Network. In constructing the model, we had to resolve the following issues: choice of appropriate subsystem, assignment of embryonic data to cellular model, choice of appropriate kinetics. Although the resulting model is capable of reproducing fractions of the experimental data, it falls short of reproducing specification of cell types. These findings can facilitate the refinement of the Endomesoderm Network.

Keywords: modeling; development; sea urchin.

1. Introduction

Development of a complex organism begins with the fertilized egg. Through a series of differential cleavages, specification events and morphological changes, the adult organism is formed. This specific and complex sequence of interconnected events requires a hard-wired plan or program, located in the genome. Together with maternal transcription factors (TFs), the genome contains all information necessary to develop to an adult organism . The single events in development are mainly mediated by differential gene expression to establish extracellular gradients in the embryo or discriminate certain cells from others [3]. Sea urchins like *Strongylocentrotus purpuratus* have been used since the end of the 19th century to study developmental processes [4]. Using modern microbiological techniques, the understanding of development of *S.purpuratus* has increased dramatically. Besides the sequence of the genome of *S.pur.* [20], a complex gene regulatory network, the Endomesoderm Network has been established that is presumed to control mesoderm and endoderm specification [2, 26]. This network, based on experimental data, is available as a graphic representation, but not as a more complex mathematical model.

A model capable of reproducing all major events and interactions in the developing sea urchin needs to be comprised of a growing number of cells in order to enable the establishment of gradients and and reproduce morphological changes. A prerequisite for such a large-scale model, though, is the existence of a working small-scale model capturing the events in one single cell.
We will show the construction of such a cellular model based on the Endomesoderm Network. Since experimental data concerning development like mRNA concentrations is, in most cases, not measured on a cellular basis but for the whole embryo and distinction between not fully specified cell types is not trivial, this modeling involves careful recalculation of experimental values. Furthermore, experimental data is very sparse so that the necessary parameter estimation becomes computationally demanding. To perform this estimation efficiently, we partition the model to minimize the number of parameters estimated simultaneously.
The result is a dynamic model that, because of its shortcomings, gives important indications for the refinement of the Endomesoderm Network.

2. Materials and Methods

The goal of this investigation was the establishment of a mathematical modeling of the processes outlined in the Endomesoderm Network. Therefore, we chose to construct a model of ordinary differential equations (ODEs) that refers to a single cell. By emulating external inputs caused by cell-cell interactions or extracellular gradients, this model should be able to reproduce experimental data. As the Endomesoderm Network focuses on the specification of different cell types, endoderm, mesoderm and primary mesenchyme cells (PMC), the model should be able to generate three distinct expression patterns.
Because of sparse available data, we chose a subset of the Endomesoderm Network for which quantitative timecourse data generally exists. This subset includes the genes *Wnt8* [23], *Otx* [10], *Blimp1* [11], *Brn* [24], *Bra* [17], *FoxA* [16], *Hox* [5], *GataE* [9], *Eve*, *Pmar1* [15] and *Notch*. We attempted to correct obvious shortcomings of the network by incorporating a model of the canonical Wnt-Pathway [7, 8].
Upon close examination, the time course data proved inadequate, since the experimental time courses are determined using all cells of the embryo. Thus, increased expression in a rather small region of the embryo following basal expression in the entire embryo would not be accounted for by the raw data. We resolved this problem by using fate maps and data from modern imaging techniques.

2.1. *Recalculation of Experimental Data*

The expression data available for the genes used in this study is determined as transcripts per embryo. It seems fairly obvious that, in a growing, developing organism, transcript number per embryo is not necessarily equal transcript number per cell. For the model constructed here, the number of transcripts per cell for each cell type is essential.

To calculate the expression of any gene per cell of a given cell type, we need information on the expression in this cell type relative to the expression in the entire embryo. This can be obtained from whole mount in situ hybridization(WISH) data, as available at [18, 27]. WISH data qualitatively determines the localization of transcripts of a given gene in the embryo.

The simplest case is that WISH data shows that a given gene is expressed in only one cell type at a given time point. The only additional information needed to calculate transcript number per cell is the number of cells comprising the given cell type. For early stages of the embryo, this can be obtained from fate maps [1, 14, 22]. For later stages, advanced imaging techniques are necessary to infer the number of cells expressing a certain marker [13, 21].

In this simple case, the number of transcripts per cell can be determined by dividing the number of transcripts at a given time point by the number of cells in the territory expressing the gene. Trivial as it sounds, this approach requires knowledge of the amount of cells expressing and transcript abundance at the same time point, which is usually not obtainable. Therefore, the number of cells in a given territory at a certain timepoint is inferred by assuming linear growth between different experimental measurements here.

In more difficult cases, i.e. a gene is expressed in multiple territories with different rates, these rates have to be approximated as good as possible from WISH data. As WISH data is rather qualitative, we assume here that genes expressed in more than one territory are expressed equally among these territories, thus the number of transcripts per embryo is divided by the number of cells of all territories expressing the gene in question.

A comparison between embryonic expression rates and recalculated expression is given in Fig.1.

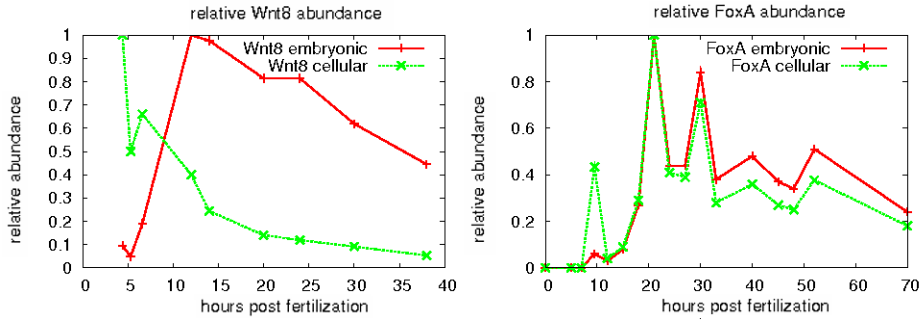

Fig. 1. Normalized Expression of Wnt8 (left panel) and FoxA (right panel), shown as expression per embryo (red) and expression per cell of expressing cell type (green). The data points are normalized to the maximum of the maximum of the respective data series.

2.2. *Details of the ODE Model*

The model was formulated as a set of ODEs. It was implemented in Systems Biology Markup Language (SBML) [6], in order to use available parameter estimation tools. To focus solely on the regulatory interactions and omit any mechanisms for which experimental data is missing, compartimentation of the model as well as transport processes are omitted. Translation and degradation reactions are modelled using first-order reaction kinetics of the form

$$v_x = k_{rt} \cdot [Y] \tag{1}$$

where x is the identifier of the reaction, k_{rt} is a constant for a given reaction type and $[Y]$ is the concentration of substrate. Transcription kinetics are formulated using a modular approach. This approach facilitates the transfer of Boolean functions to ODE models: A given TF can have an activating or an inhibiting influence on its target gene's expression. An activatory influence is of TF A on gene G is defined as

$$\varphi_{G_A} = \frac{k_{A_G} \cdot [A]}{c_{A_G} + [A]} \tag{2}$$

whereas an inhibitory input of TF I on G is given by

$$\varphi_{G_I} = \frac{k_{I_G} \cdot c_{I_G}}{c_{I_G} + [I]} \tag{3}$$

with k_{A_G}, c_{A_G}, k_{I_G} and c_{I_G} parameters specific for each distinct combination of TF and effected gene.

To further exemplify, consider the case of some gene G, activated by TF *A1* as well as *A2*, both acting additively. The formalism above combined with a degradation term yields

$$\frac{d[G_{mRNA}]}{dt} = \frac{k_{A1_G} \cdot [A1]}{c_{A1_G} + [A1]} + \frac{k_{A2_G} \cdot [A2]}{c_{A2_G} + [A2]} - k_{deg\_mRNA} \cdot [G_{mRNA}] \tag{4}$$

Using k_{A1_G},c_{A1_G},k_{A2_G} and c_{A2_G}, the strength of each input can be controlled independently. Obviously, this formalism introduces a rather large number of parameters, but these are necessary to allow for different activatory and inhibitory strengths of one TF on different genes and different contributions of multiple TFs to the expression of one gene. The rate laws of this formed used in this model are given in Table 1.

Any number of inputs of both types can be combined using multiplication in case the influence of all TFs is necessary to produce output or using addition in the case that the influence of either one of the TFs is required. Such a combination is then used as the velocity of a given transcription reaction.

Most parameters in the resulting set of ODEs are undetermined and cannot be obtained from literature, necessitating parameter estimation. We chose SBML-PET [25] to estimate these parameters.
Since most parameters depend, directly or indirectly, on other parameters, estimation of all parameters simultaneously is computationally nearly infeasible. We therefore partitioned the model into submodels, emulating necessary inputs according to experimental data, and estimated the parameters in small groups.
Therefore and to mimic transcriptional regulation arising from extracellular gradients, we made use of event structures provided in SBML. Event structures do have the unfavorable characteristic to introduce discontinuous elements in the system of ODEs. We therefore constructed a formula that consists of the sum of an activatory Hill-Kinetic and an inhibitory Hill-Kinetic. Only one of the two summands is active at a time, depending on whether the modeled concentration is rising (activatory term) or declining (inhibitory term). The activity of either term and the parameters involved are controlled using events. The change in concentration of x is given by

$$\frac{d[x]}{dt} = S_1 \cdot k \cdot \frac{t^h}{\Theta^h + t^h} \; + \; (1 - S_1) \cdot k \cdot (1 - \frac{t^h}{\Theta^h + t^h}) - k_{deg} \cdot [x] \qquad (5)$$

Here, k is used to control the maximum concentration of x, t is simulation time, Θ equals the value of t where x reaches half of its maximal value, h is the hill coefficient controlling the steepness of the slope and $-k_{deg} \cdot [x]$ is a degradation term.
S_1 controls whether the concentration of x is rising or falling. Requiring $S_1 \in \{0, 1\}$, either the first or the second summand in Eq. 5 are non-zero. Reseting S_1 and fine-tuning of the other parameters using events enables the reproduction of complex temporal patterns without discontinuities.

3. Results

As quantitative time courses of mRNA concentrations for most genes in the Endomesoderm Network are very sparse, we selected genes for which detailed experimental data is available. These genes are also the presumed key genes of the network. A graph representation of the resulting network is given in Fig.2.
As explained before, the difference between different genes arises from differences in transcriptional regulation alone. Hence, the rate laws controling transcription are given in Table 1 along with the general kinetics used for the other reactions. To drive differential expression in the different cell types, the helper variables $Notch$, TCF_REP, $meso\_REP$, $PMC\_repressor$ and Otx_REP are used. Their activities are shown in Table 2. The activities are given at the mRNA level and as protein degradation is slower than mRNA degradation, protein abundance lasts longer.
Further details of the ODE model, like those concerning the Wnt-Pathway model included in the model can be obtained from the SBML file in supplemental data.
Simulation results of the model were compared to experimentally determined and recalculated time courses. The two sets are compared in Fig.3. In general, the simu-

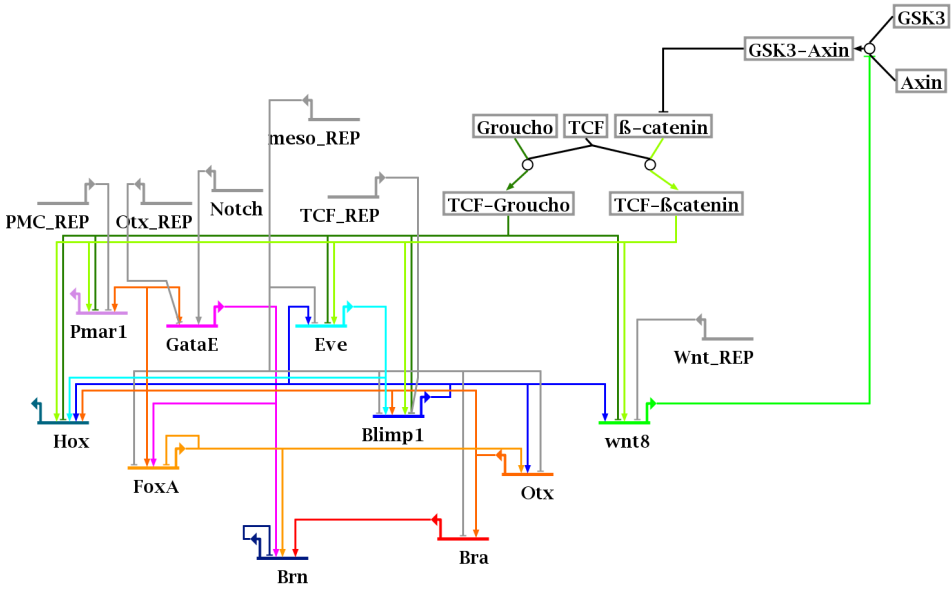

Fig. 2. Topology of the Boolean model underlying the model analyzed here. Arrows indicate activatory interactions, barred lines indicate inhibitory interactions. Genes are represented as horizontal lines with arrows, proteins and protein complexes as rectangles. Helper variables (grey genes) represent influences necessary for the boolean network to reproduce experimnetal data that are not based on any experimental data or assumptions. Note all helper variables have inhibitory effects. Figure created using Biotapestry [12]

Table 1. Rate laws for transcriptional regulation and general kinetics

ne/Reaction	Rate Law
Blimp1	$(\frac{3.506\cdot[bcat\_TCF]}{1.118+[bcat\_TCF]} + \frac{1.0\cdot[Otx]}{(0.5397+[Otx])} + \frac{1.0\cdot[Eve]}{100.0+[Eve]}) \cdot (\frac{2.073\cdot 1.0}{1.0+[Gro\_TCF]} + \frac{1.0\cdot[TCF\_REP]}{100+[TCF\_REP]}) \cdot \frac{1.0\cdot 1.0}{1.0+[meso\_REP]}$
Bra	$\frac{7.366\cdot[Otx]}{100.0+[Otx]} \cdot \frac{14.89\cdot 0.13}{0.13+[Otx\_REP]} \cdot \frac{5.475\cdot 71.91}{71.91+[meso\_REP]}$
Brn	$\frac{1.942\cdot[GataE]}{1.942+[GataE]} \cdot \frac{25.0\cdot[FoxA]}{700.0+[FoxA]} \cdot \frac{25.0\cdot[Bra]}{700.0+[Bra]} \cdot \frac{2.0\cdot 1.0}{2.0+[Brn]}$
Eve	$\frac{3.22\cdot[Blimp1]}{0.1+[Blimp1]} \cdot \frac{6.586\cdot[bcat\_TCF]}{100.0+[bcat\_TCF]} \cdot \frac{34.29\cdot 0.1}{0.1+[Gro\_TCF]} \cdot \frac{1.0\cdot 1.0}{1.0+[meso\_REP]}$
FoxA	$((\frac{2.035\cdot[Otx]}{0.1+[Otx]} \cdot \frac{4.534\cdot 5.804}{5.804+[Otx\_REP]} + \frac{43.49\cdot[GataE]}{10.61+[GataE]}) \cdot \frac{1.001\cdot 5.0}{5.0+[meso\_REP]} + (\frac{2.035\cdot[Otx]}{0.1+[Otx]} \cdot \frac{4.534\cdot 5.804}{5.804+[Otx\_REP]})) \cdot \frac{1.001}{100.0+}$
GataE	$\frac{4.958\cdot[Otx]}{0.1+[Otx]} \cdot \frac{1.0\cdot 1.384}{1.384+[Otx\_REP]} + \frac{2.982\cdot[Notch]}{100.0+[Notch]}$
Hox	$(\frac{100.0\cdot[bcat\_TCF]}{13.98+[bcat\_TCF]} + \frac{1.0\cdot[Eve]}{100.0+[EvepMC]} + \frac{1.0\cdot[Blimp1]}{100.0+[Blimp1]}) \cdot \frac{1.0\cdot 0.1}{0.1+[Gro\_TCF]} \cdot \frac{1.0\cdot[Otx]}{0.2236+[Otx]}$
Otx	$(\frac{14.62\cdot[GataE]}{0.1752+[GataE]} \cdot \frac{1.0\cdot[FoxA]}{1.0+[FoxA]} + \frac{11.06\cdot[Blimp1]}{7.275+[Blimp1]}) \cdot \frac{1.0\cdot 1.0}{1.0+[meso\_REP]}$
Pmar1	$\frac{3.408\cdot[Otx]}{0.1+[Otx]} \cdot \frac{37.24\cdot[bcat\_TCF]}{100.0+[bcat\_TCF]} \cdot \frac{29.08\cdot 0.1}{0.1+[Gro\_TCF]} \cdot \frac{1.0\cdot 1.0}{1.0+[pmc\_REP]}$
Wnt8	$(\frac{2.644\cdot[bcat\_TCF]}{99.92+[bcat\_TCF]} + \frac{29.64\cdot[Blimp1]}{0.3815+[Blimp1]}) \cdot \frac{7.164\cdot 0.1}{0.1+[Wnt\_REP]} \cdot \frac{10.4\cdot 0.1}{0.1+[Gro\_TCF]}$
$\iota dation_{mRNA}$	$0.2 \cdot [X_{mRNA}]$
$\iota anslation$	$2.0 \cdot [X_{mRNA}]$
$dation_{X_{protein}}$	$0.10193 \cdot [X]$

Table 2. Period of activity of helper variables in different territories. Cells values pertain to the values of $\Theta_{activatory}$ and $\Theta_{inhibitory}$ in Equation 5

Variable	Endoderm	Mesoderm	PMC
PMC_{REP}	OFF	$START : END$	$START : END$
$meso_{REP}$	$8 : END$	$15 : END$	OFF
TCF_{REP}	OFF	OFF	$24 : END$
Otx_{REP}	$START : 10$	$Start : 17$	$Start : 17$
Wnt_{REP}	$10 : END$	$10 : END$	$10 : END$

lation results are –at least– qualitatively similar to the experimental data, although the time scale is not equivalent among all genes. One exception is FoxA, which shows oscillating behavior not reproduced by the model.

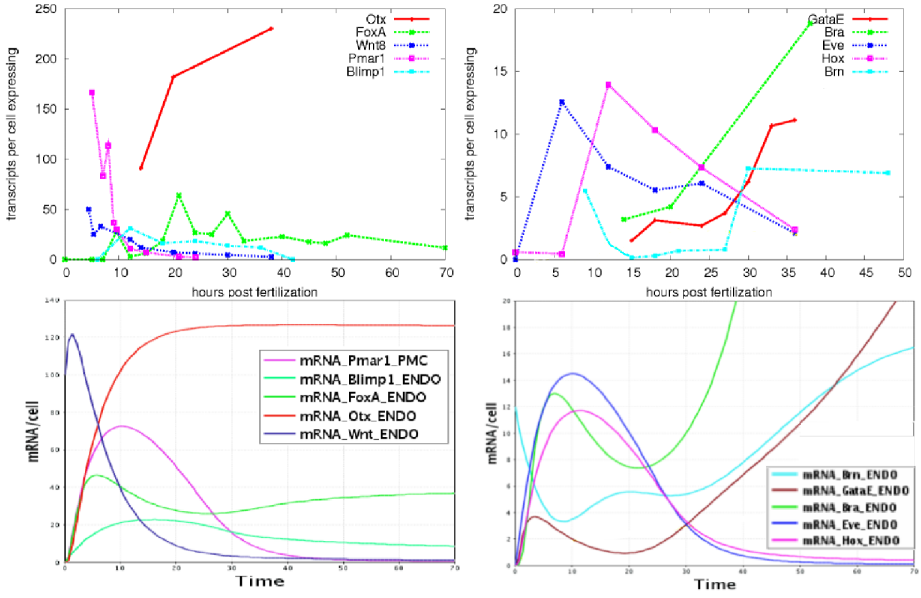

Fig. 3. Time courses as determined from experimental data (top row) and simulation results (bottom row). To determine transcripts/cell, we assumed that each gene is expressed in one cell type only but equally throughout this cell type. Therefore, the expression of each gene is shown for only one cell type (Endoderm for Blimp1, FoxA, Otx, Wnt, Brn, GataE, Bra, Eve, Hox; PMC for Pmar1). In the recalculated experimental data, transcript abundance in other cell types is assumed to be 0. In simulation results, this clear distinction between cell types could not be obtained.

In general, the designed model reproduces the available experimental data to a satisfying extend.

4. Discussion

The present analysis highlights a few issues arising when modeling developmental GRNs. These issues do not include evaluation or analysis of the resulting model itself. As most methods to analyze models require a steady state, which is not necessarily given or of interest in developmental processes, the analysis of developmental GRNs poses new challenges here as well.

The issues addressed in this study can be summarized as: dealing with sparse experimental data and choosing kinetics for transcriptional regulation. We will briefly discuss the approaches undertaken here to solve these issues before we critically evaluate the model constructed here.

As shown in Sec. 2.1, the available embryonic data needs recalculation to cellular data. We perform such a recalculation by using WISH data to determine spatial expression and different data containing counts of cell numbers for different embryonic territories and time points. From this data, we can infer the number of cells expressing a given gene and thus determine the cellular expression from embryonic expression data. This recalculation crucially depends on data that is very sparse as of today and definitely needs refinement.

The point we want to stress here is that this conversion to cellular data is vital for most modeling approaches concerned with development. Thus, existing experimental data is not necessarily as extensive as it seems at first sight.

The transcriptional kinetics chosen here represent a versatile and intuitive way to connect the regulatory input to the gene to the resulting output in terms of transcription.

The parameters used in these kinetics do not necessarily resemble biochemical constants measurable in experiments.

Using the estimated parameters, the model can be used to simulate the time course and validate the results by comparison to experimental data. The simulated time courses of each gene generally resemble the experimentally determined time course for the cell type expressing the gene.

Nevertheless, the genes are not efficiently shut off in the cell types that are not supposed to express the gene in question. This is most probably due to a lack in inhibitory interactions in the model. Since these interactions are not to be found in the underlying Endomesoderm Network, the need for the refinement of both networks, the Endomesoderm Network and the model presented here, becomes obvious. For the refinement of the networks, new experimental data as well as a reassessment of the existing data is inevitable.

As the Endomesoderm Network contains many features which are believed to be conserved throughout evolution, experimental findings from other species can be an important source of additional information. One example could be the recent findings on non-canonical Wnt-signaling in Xenopus [19].

5. Conclusion

We have successfully created an ODE model on the basis of the Endomesoderm Network. Although this model is not capable of correctly reproducing specification of cells, the present analysis highlights some issues arising in modeling of large developmental GRNs. We hope to thereby improve alertness of computational as well as experimental researchers for the requirements for modeling large developmental GRNs.

The Endomesoderm Network itself must be understood as a snapshot of ongoing research which is constantly refined. Thus, we hope to aid in this refinement by presenting this detailed model of the key components of the network and highlighting the lack of inhibitory interactions.

Supporting Data

Supporting data includes SBML-version of the model

Acknowledgments

We would like to thank Christoph Wierling and Alexander Kühn for fruitful discussion. Clemens Kühn is funded by German Research Foundation via the International Research Training Group "Genomics and Systems Biology of Molecular Networks".

References

[1] Dan, K., Tanaka, S., Yamazaki, K., Kato, Y., Cell cycle study up to the time of hatching in the embryos of the sea urchin, hemicentrotus pulcherrimus, *Development Growth and Differentiation*, 22(3):589–598, 1980.

[2] Davidson E.H., et al, A Provisional regulatory gene network for specification of endomesoderm in the sea urchin embryo, *Dev. Biol.*, 246(1):162–190, 2002.

[3] Davidson, E.H., Erwin, D.H., Gene regulatory networks and the evolution of animal body plans, *Science*, 311(5762):796–800, 2006.

[4] Hertwig, O., Beiträge zur Kenntnis der Bildung, Befruchtung und Teilung des tierischen Eies, *Gegenbaurs Morphologisches Jahrbuch*, 1:374–452, 1876.

[5] Howard-Ashby, M., Materna, S. C., Brown, C. T., Chen, L., Cameron, R.A., Davidson E. H, Identification and characterization of homeobox transcription factor genes in Strongylocentrotus purpuratus, and their expression in embryonic development, *Dev. Biol.*, 300(1):74–89, 2006.

[6] Hucka, M., et al., The Systems Biology Markup Language (SBML): A Medium for Representation and Exchange of Biochemical Network Models, *Bioinformatics*, 19(4):524–531, 2003.

[7] Krüger, R., Heinrich R., Model reduction and analysis of robustness for the Wnt/β-Catenin signal transduction pathway, *Genome Inform.*, 15(1):138–148, 2004.

[8] Lee, E., Salic, A., Krüger, R., Heinrich, R., Kirschner M.W., The roles of APC and Axin derived from experimental and theoretical analysis of the Wnt pathway, *PLoS Biology*, 1(1):116, 2003.

[9] Lee, P.Y., Davidson, E.H., Expression of Spgatae, the Strongylocentrotus purpuratus ortholog of vertebrate GATA4/5/6 factors, *Gene Expr. Patterns*, 5(2):161–165, 2004.

[10] Li, X., Chuang, C.-K., Mao, C.-A., Angerer, L.M., Klein, W.H., Two Otx Proteins Generated from Multiple Transcripts of a Single Gene in Strongylocentrotus purpuratus, *Dev. Biol.*, 187(2):253–266, 1997.
[11] Livi, C.B., Davidson E.H, Expression and function of blimp1/krox, an alternatively transcribed regulatory gene of the sea urchin endomesoderm network, *Dev. Biol.*, 293(2):513–525, 2006.
[12] Longabaugh, W.J.R., Davidson, E.H., Bolouri, H., Computational representation of developmental genetic regulatory networks, *Dev. Biol.*, 283(1):1–16, 2005.
[13] Martins, G.G., Summers, R.G., Morill, J.B., Cells are added to the archenteron during and following secondary invagination in the sea urchin lytechinus variegatus, *Dev. Biol.*, 198:330–342, 1998.
[14] Masuda, M., Sato, H., Asynchronization of cell division is concurrently related with ciliogenesis in sea urchin blastulae. *Development Growth and Differentiation*, 26(33):281–294, 1984.
[15] Oliveri, P., Carrick, D.M., Davidson, E.H., A Regulatory Gene Network That Directs Micromere Specification in the Sea Urchin Embryo, *Developmental Biology*, 246(1):209–228, 2002.
[16] Oliveri, P. , Walton, K.D., Davidson, E.H., McClay, D.R., Repression of mesodermal fate by foxa, a key endoderm regulator of the sea urchin embryo, *Development*, 133(21):4173–4181, 2006.
[17] Poustka, A.J., Kühn, A., unpublished results
[18] Poustka, A.J., Kühn, A., Groth, D., Weise, V., Yaguchi, S., Burke, R.D., Herwig, R., Lehrach, H., Panopoulou, G., A global view of gene expression in lithium and zinc treated sea urchin embryos: new components of gene regulatory networks, *Genome Biol.*, 8(5):R85, 2007
[19] Schambony,A., Wedlich, D., Wnt-5A/Ror2 Regulate Expression of XPAPC through an Alternative Noncanonical Signaling Pathway, *Developmental Cell*, 12:779–792, 2007.
[20] Sea Urchin Genome Sequencing Consortium, The Genome of the sea urchin Strongylocentrotus Purpuratus, *Science*, 314:941–953, 2006
[21] Summers, R.G., Morill, J.B., Leith, J., Marko, M., Piston, D.W., Stonebraker, A.T., A stereometric analysis of karyokinesis, cytokinesis and cell arrangements during and following fourth cleavage period in the sea urchin, Lytechinus Variegatus, *Development Growth and Differentiation*, 35(11):41–57, 1993.
[22] Tanaka, S., Dan, K., Study of the lineage and cell cycle of small micromeres in the embryos of the sea urchin, Hemicentrotus pulcherrimus, *Development Growth and Differentiation* 32(2):145–156, 1990.
[23] Wikramanayake, A.H., Peterson, R., Chen, J., Huang, L., Bince, J.M., McClay,D.R., Klein, W.H., Nuclear β-Catenin-Dependent Wnt8 Signaling in Vegetal Cells of the Early Sea Urchin Embryo Regulates Gastrulation and Differentiation of Endoderm and Mesodermal Cell Lineages, *Genesis*, 39(3):194–205, 2004.
[24] Yuh, C.-H., Dorman, E.R., Davidson, E.H., Brn1/2/4, the predicted midgut regulator of the endo16 gene of the sea urchin embryo, *Dev. Biol.* 281(2):286–298, 2005.
[25] Zi, Z., Klipp, E., SBML-PET: a systems biology markup language based parameter estimation tool, *Bioinformatics*, 22(21):2704–2705, 2006.
[26] `http://sugp.caltech.edu/endomes/`
[27] `http://goblet.molgen.mpg.de/eugene/cgi/eugene.pl`